Continuum Mech. Thermodyn. (2021) 33:1621–1636
https://doi.org/10.1007/s00161-021-00997-2

ORIGINAL ARTICLE

Y. Espinosa-Almeyda · R. Rodríguez-Ramos · H. Camacho-Montes · R. Guinovart-Díaz · F. J. Sabina

Elliptic functions and lattice sums for effective properties of heterogeneous materials

Received: 30 October 2020 / Accepted: 2 March 2021 / Published online: 24 March 2021

Abstract Effective properties of fiber-reinforced composites can be estimated by applying the asymptotic homogenization method. Analytical solutions are possible for infinite long circular fibers based on the elliptic quasi-periodic Weierstrass Zeta function. This process leads to numerical convergences issues related to lattice sums calculations. The lattice sums original series converge slowly, which make the calculation difficult. This problem needs to be addressed because effective properties are highly sensitive to these values. Therefore, a systematic review and analysis for the lattice sums are a necessity. In the present work, the Eisenstein–Rayleigh lattices sums are reviewed and numerically implemented for fiber-reinforced composites with parallelogram unit periodic cell whose fibers are centered, or not, at the coordinate origin. Numerical values are reported and compared with available data in the literature obtaining good agreements. In this work, new Eisenstein–Rayleigh lattice sums are obtained that are easy to implement and a set of tables with numerical values are given.

Keywords Lattice sums · Asymptotic homogenization method · Elliptic Weierstrass function · Parallelogram periodic unit cell

1 Introduction

The development of analytical mathematical models and numerical approaches to predict the effective properties (such as Young's modulus, shear, conductivity, permittivity, piezoelectricity, magnetoelectric coupling and others) of advance heterogeneous multiphase composites is still important for applications. Some of the developed models are based on the Mori–Tanaka method [1–3], self-consistent schemes [4], eigenfunction

Communicated by Marcus Aßmus, Victor A. Eremeyev and Andreas Öchsner.

R. Rodríguez-Ramos (✉) · R. Guinovart-Díaz
Facultad de Matemática y Computación, Universidad de La Habana, San Lázaro y L, 10400 La Habana, Cuba
E-mail: reinaldo@matcom.uh.cu

R. Rodríguez-Ramos
Escuela de Ingeniería y Ciencias, Tecnológico de Monterrey, Campus Puebla Atlixcáyotl 5718, Reserva Territorial Atlixcáyotl, 72453 Puebla, Mexico

Y. Espinosa-Almeyda · H. Camacho-Montes
Instituto de Ingeniería y Tecnología, Universidad Autónoma de Ciudad Juárez, Av. del Charro 610 Norte, 32310 Ciudad. Juárez, Chihuahua, Mexico

Y. Espinosa-Almeyda · F. J. Sabina
Instituto de Investigaciones en Matemáticas Aplicadas y en Sistemas, Universidad Nacional Autónoma de México, Apartado Postal 20-126, Alcaldía Álvaro Obregón, 01000 Mexico City, CDMX, Mexico

expansion-variational method [5], the finite element [6,7] and the homogenization [8–12] methods. Fundamentally, the mathematical framework of these models is given by a set of partial differential equations with rapidly oscillating coefficients and subject to boundary and interface conditions, which characterize the constituent physical properties, phase distribution and shape of the composite materials. It is desirable to quickly solve the resulting boundary-value problems.

For periodic composite structures, such as fiber-reinforced composites (FRCs), elliptical boundary-value problems are often found, see, for instance, Refs. [13,14]. Solutions for these elliptical boundary-value problems have been implemented by means of the homogenization methods using different mathematical techniques [14–19]. A two-scale asymptotic expansion-based approach is developed in Refs. [9,20–25]. In these works, the two-scale asymptotic homogenization method (AHM) based on complex potentials through doubly periodic Weierstrass' elliptic functions is applied to find exact analytical or semi-analytical solutions. Analytical solutions are determined as a function of the quasi-periodic Weierstrass Zeta and Natanzon's functions and related ones, which require the lattice sums calculation at an origin-centered point inside of the periodic cell, see Refs. [9,13,22,26–29].

The AHM application to calculate the effective properties of multiphase periodic FRCs with two or more different fibers within a double periodic array is a goal to be solved. For example, the effective transverse shear modulus is calculated by AHM for a hybrid unidirectional FRC with three isotropic phases; herein, one fiber is assumed to be centered at the origin and other one is not; both are embedded in a matrix [30]. The effective conductivity is estimated for a FRC with rectangular periodic array of unidirectional and perfectly conducting cylinder pairs in a uniform host by Rylko [31]. Effective transport properties of multiphase FRCs with a doubly periodic square, hexagonal and triangular arrays of fiber pairs via complex variable method are reported in [32]. Mityushev calculated the effective conductivity of two-dimensional two-phase periodic composite with a non-overlapping unidirectional and identical circular disk within a matrix by means of doubly periodic elliptic functions using the Eisenstein series [33]. In particular, for this type of multiphase FRCs, to find the solution via AHM through the doubly periodic Weierstrass' elliptic functions by Laurent and Taylor expansions requires calculating the lattice sums at any point $z = z_1$ inside of the periodic cell Y. Therefore, to calculate the lattice sums at any point $z = z_1$ inside of the periodic cell Y is the aim of this work. The analysis of the effect of multiples non-concentric fibers and its interaction on effective properties of periodic FRCs is a topic that requires further attention.

In the classical work of Rayleigh, the conductivity of a periodic two-phase media reinforced by unidirectional cylinders is analyzed and a well-established formulation to calculate the lattice sums is reported [34]. Since then, different procedures for evaluating the lattice sums have been implemented. For example, Berman and Greengard proposed a renormalization method to calculate the lattice sums [35]. Huang presented two- and three-dimensional integral formulations for the harmonic lattice sums [36]. C. B. Ling reported the evaluation of Weierstrass' elliptic function at half periods for rectangular [37], rhombic [38] and parallelogram [39] primitive periodic cells. Tables of lattice sums values relating to Weierstrass' elliptic function are also given by C. B. Ling [40]. Expressions for the doubly periodic Green's tensors in elastostatic and elastodynamic problems and the related lattice sums were calculated using the Fourier transform method as shown by Movchan et al. [41]. In addition, Rayleigh's identities through Lame potentials in terms of Bessel functions were shown for static and dynamic problems [41]. Eisenstein-type sums have been very useful in the analysis of effective properties of doubly periodic composites [42–45]. Explicit formulas for generalized Eisenstein series are given in Ref. [46]. In addition, displaced lattices of high symmetry are also analyzed via geometric multiset identities as function of origin-centered lattice sums. Recently, a review of some of the most important analytic techniques to obtain the lattice sums is outlined in Borwein et al. [47]. Closed-form formulas for the lattice sums of two-dimensional composites in terms of elliptic integrals for conductivity (S_2) and for elasticity (T_2) are established in Yakubovich et al. [48].

The main contribution of this work is to systematize the Eisenstein–Rayleigh lattice sums calculations. The computation of effective properties is highly sensitive to Eisenstein–Rayleigh lattice sums, so that reliable numbers are of great importance. However, the available numerical data in the literature are somehow limited. Therefore, it is necessary to compile these values and develop methods for the comparison and application of them in composite materials. In this work, the analytical formulae of the Eisenstein–Rayleigh lattice sums S_{k+p} and E_{k+p} are determined for parallelogram periodic cells whose fibers are centered, or not, at the coordinate origin, respectively, following the procedure developed by Lord Rayleigh [34]. It generalizes the well-established Rayleigh methodology obtained for square and rectangular periodic cells. In addition, an alternative method is implemented to compute the Eisenstein sums E_{k+p} by combining the Rogosin's Eisenstein series representation in the form of a power series [43] with Rayleigh's procedure applied to the sum values

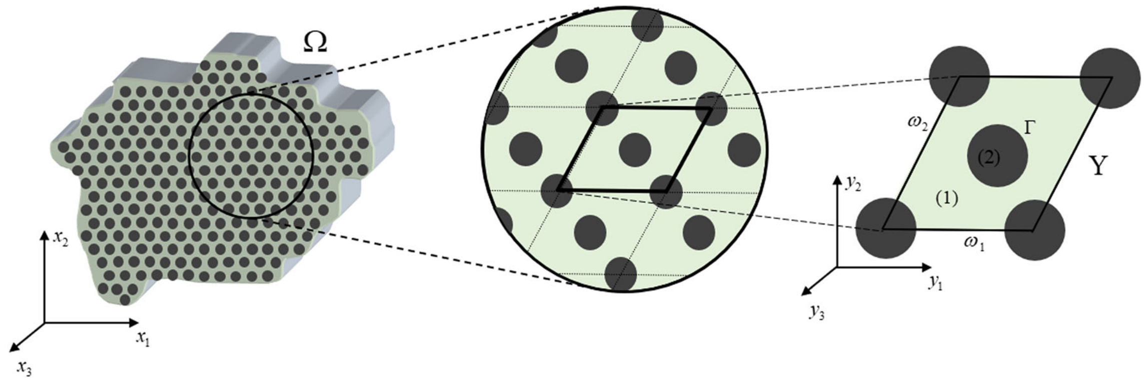

Fig. 1 Heterogeneous periodical structure Ω (left), blow-up (middle) and parallelogram periodic unit cell Y of periods ω_1 and ω_2, and principal angle θ (right)

S_{k+p} for parallelogram periodic cell. Tables of new Eisenstein–Rayleigh lattice sum values are reported for square, rectangular and parallelogram periodic cells whose fibers are centered, or not, at the coordinate origin. Finally, a wider variety of unit cells for periodic composite can be studied. Comparisons with other sum values reported in literature are also analyzed.

2 Weierstrass elliptic functions in a linear elasticity problem of a heterogeneous structure

In linear elasticity, a static elliptic boundary value problem for a heterogeneous periodical structure Ω (Fig. 1) can be stated by the equilibrium linear equation

$$\sigma_{ij,j} = 0, \quad \text{in } \Omega, \tag{1}$$

with the boundary conditions

$$u_k|_{\partial\Omega_u} = g_0, \; \sigma_{ij}\, n_j \big|_{\partial\Omega_\sigma} = T_0, \qquad \text{on} \quad \partial\Omega = \partial\Omega_u \cup \partial\Omega_\sigma, \tag{2}$$

and perfect interface conditions

$$[[\, u_k \,]] = 0, [[\, \sigma_{ij}\, n_j \,]] = 0, \qquad \text{on } \Gamma, \tag{3}$$

In Eqs. (1)–(3), σ_{ij} and u_k are the stress and the displacement components, respectively. They are related by Hooke's law $\sigma_{ij} = C_{ijkl}\, \varepsilon_{kl}$ and strain–displacement relation $\varepsilon_{kl} = (u_{k,l} + u_{l,k})/2$ where C_{ijkl} is the elastic stiffness coefficients with $i,\ j,\ k,\ l = 1,\ 2,\ 3$. The comma notation means partial differentiation, i.e., $f_{i,j} = \partial f_i/\partial x_j$. Also, g_0 and T_0 are the prescribed displacement and stress on $\partial\Omega$ boundary of Ω, and Γ denotes the interface matrix-fiber. The notation $[[\, f \,]] = 0$ represents the continuity of f across the interface Γ. In addition, the elastic stiffness coefficients C_{ijkl} satisfy the following symmetries,

$$C_{ijkl} = C_{jikl} = C_{ijlk} = C_{klij}, \tag{4}$$

and the positivity condition for all $\mathbf{x} \in \Omega$, i.e.,

$$\exists\, \eta > 0, \quad C_{ijkl}\, (\mathbf{x}/\varepsilon)\, a_{ij} a_{kl} \geq \eta a_{ij} a_{kl}, \tag{5}$$

for any a_{ij} symmetric 3×3 matrix.

Note that in Fig. 1 there are two coordinate systems representing two scales: the composite characteristic size L and the size l of the periodic cell Y. Herein, the slow- and fast-scale relation $\mathbf{y} = \mathbf{x}/\varepsilon$ is given by the small parameter $\varepsilon = l/L$ with $\varepsilon << 1$.

The asymptotic solution of the elliptic boundary value problem (Eqs. (1)–(3)) via two-scale asymptotic homogenization method (AHM) has been used in Refs. [9,10,21], by posing the Ansatz:

$$u_k\, (\mathbf{x}) = u_k^{(0)}\, (\mathbf{x}, \mathbf{y}) + \varepsilon u_k^{(1)}\, (\mathbf{x}, \mathbf{y}) + O\left(\varepsilon^2\right), \tag{6}$$

in powers of the small parameter ε. Upon the application of AHM, it is found that $u_k^{(0)}(\mathbf{x},\mathbf{y}) \equiv u_k^{(0)}(\mathbf{x})$, i.e., it only depends on the slow variable $\mathbf{x}$ and $u_k^{(1)}(\mathbf{x},\mathbf{y})$ is a Y-periodic functions with respect to the fast variable $\mathbf{y}$. Also, the function $u_k^{(1)}(\mathbf{x},\mathbf{y})$ can be obtained by separating the variables $\mathbf{x}$ and $\mathbf{y}$, as $u_k^{(1)}(\mathbf{x},\mathbf{y}) = {}_{pq}N_k(\mathbf{y})\left(\partial u_p^{(0)}(\mathbf{x})/\partial x_q\right)$ where ${}_{pq}N_k(\mathbf{y})$ is the solution of the so-called local problems, defined as ${}_{pq}\mathcal{L}$.

Thus, substituting Eq. (6) into Eqs. (1)–(3), a set of recurrent problems defined by a set of differential equations and interface conditions is obtained in relation to the power of ε parameter. This way, the mathematical statement of the so-called local problems ${}_{pq}\mathcal{L}$, the equivalent homogenized problem and analytical formulas for the effective coefficients can be found, see Refs. [9,29], as follows:

${}_{pq}\mathcal{L}$ local problems,

$$\left(C_{ijkl}^{(\gamma)}\,{}_{pq}N_{k,l}^{(\gamma)}\right)_{,j} = -\left(C_{ijpq}^{(\gamma)}\right)_{,j}, \qquad \text{in Y}, \tag{7}$$

$$[[\,{}_{pq}N_k\,]] = 0,\ [[\,C_{ijpq}n_j + C_{ijkl}\,{}_{pq}N_{k,l}n_j\,]] = 0, \ \text{on } \Gamma, \tag{8}$$

$$\left\langle {}_{pq}N_k \right\rangle = 0. \tag{9}$$

Homogenized problem on equivalent medium $\bar{\Omega}$,

$$C_{ijpq}^{*}\frac{\partial^2 u_p^{(0)}(\mathbf{x})}{\partial y_j \partial y_q} = 0, \qquad \text{on } \bar{\Omega}, \tag{10}$$

$$u_k^{(0)}\Big|_{\partial\bar{\Omega}_u} = \bar{g}_0,\ \bar{\sigma}_{ij}n_j\,\big|_{\partial\bar{\Omega}_\sigma} = \bar{T}_0, \qquad \text{on } \partial\bar{\Omega} = \partial\bar{\Omega}_{\bar{u}} \cup \partial\bar{\Omega}_{\bar{\sigma}}, \tag{11}$$

and the effective coefficients

$$C_{ijpq}^{*} = \left\langle C_{ijpq} + C_{ijkl}\,{}_{pq}N_{k,l}\right\rangle, \tag{12}$$

where $\bar{g}_0$ and $\bar{T}_0$ are the average prescribed displacement and stress on $\partial\bar{\Omega}$ boundary of $\bar{\Omega}$, and $\langle f\rangle = (1/|\mathrm{Y}|)\int_{\mathrm{Y}} f(y)\,\mathrm{dY}$ is the volume average per unit length in the periodic cell Y. The dependence of variable y is omitted for simplicity.

The theoretical details and mathematical procedures for the deduction of this recurrent problems by AHM are well described in Refs. [1,5–9] and for coupled field problems on multiphase composites are also reported in Refs. [8,22,24,29,49–52]. Herein, these procedures are omitted.

By means of complex variable theory, the ${}_{pq}\mathcal{L}$ local problems are solved considering the complex-potential method. The doubly periodic Weierstrass' elliptic functions have been useful to develop analytical solutions for this problem, mainly in heterogeneous multiphase elastic structures reinforced by unidirectional circular fibers embedded in a matrix with parallelogram periodic cell Y, see, for instance, Refs. [26,53]. Commonly, the double periodic solution ${}_{pq}N_k$ of the ${}_{pq}\mathcal{L}$ local problems is found by means of complex potential as a function of $z = y_1 + iy_2$ on Y, in terms of Laurent and Taylor expansions for ${}_{pq}N_k$ on Γ, which depend on the double periodic elliptic Weierstrass function $\wp(\omega_1,\omega_2;z)$ with periods ω_1 and ω_2. This solution can also be expressed in terms of the quasi-periodic Weierstrass Zeta function $\zeta(\omega_1,\omega_2;z)$, Natanzon's function $Q(\omega_1,\omega_2;z)$ and its derivates [9,13,22,26–30].

There are multiphase periodic FRCs where the reinforcements may have a certain distribution where some of them are not located at the coordinate origin, for instance, periodic cell cross section of diamond type with periods ω_1 and ω_2 (see Fig. 1) [30,54]. This situation may require calculating the lattice sums at any point $z = z_1$ inside of the periodic cell Y to find the ${}_{pq}\mathcal{L}$ local problems solution.

Then, the Weierstrass function $\wp(\omega_1,\omega_2;z-z_1)$ and the quasi-periodic Weierstrass Zeta function $\zeta(\omega_1,\omega_2;z-z_1)$ with poles at $z = z_1$ on the cell Y are written as follows:

$$\wp(\omega_1,\omega_2;z-z_1) = \frac{1}{(z-z_1)^2} + \sum_{s,t}{}' \left\{\frac{1}{(z-z_1-\beta_{st})^2} - \frac{1}{\beta_{st}^2}\right\}, \tag{13}$$

$$\zeta(\omega_1,\omega_2;z-z_1) = \frac{1}{z-z_1} + \sum_{s,t}{}' \left\{\frac{1}{z-z_1-\beta_{st}} + \frac{1}{\beta_{st}} + \frac{z-z_1}{\beta_{st}^2}\right\}, \tag{14}$$

where $\beta_{st} = s\omega_1 + t\omega_2$ with $s, t \in \mathbb{Z}$ represent the period lattice. The summation symbol $\sum_{s,t}'$ means that the summation does not include the point $(s, t) = (0, 0)$. In addition, it is satisfied that $\zeta'(\omega_1, \omega_2; z - z_1) = -\wp(\omega_1, \omega_2; z - z_1)$ for all $z \in \mathbb{C}$ and $\lim_{z-z_1\to 0}\left[\zeta(\omega_1, \omega_2; z - z_1) - \frac{1}{z-z_1}\right] = 0$.

From Eqs. (13) and (14), following the methodology developed in Ref. [28,43,55], we have that $\wp(\omega_1, \omega_2; z)$, $\zeta(\omega_1, \omega_2; z)$ and its derivates at the point $z = z_1$ are defined as functions of the Eisenstein–Rayleigh lattice sums S_{k+p} and $E_{k+p}\,(z - z_1)$ for $k + p \geq 2$, such as

$$S_{k+p}(\omega_1, \omega_2) = \sum_{s,t}{}' \frac{1}{\beta_{st}^{(k+p)}} \qquad \text{for } \delta = 0, \tag{15}$$

where $S_{k+p} = 0$ for $k + p$ is an odd positive integer number, and

$$E_{k+p}(\omega_1, \omega_2; z - z_1) = \sum_{s,t} \frac{1}{(z - z_1 - \beta_{st})^{(k+p)}}, \tag{16}$$

at any point $z = z_1$.

Note that the lattice sums E_{k+p} defined here are different from those formulated in Ref. [32]. A generalized formula that relates E_{k+p} as function of S_{k+p} is given in Eq. (47) of Ref. [43].

The lattice sums S_{k+p} and E_{k+p} (Eqs. (15) and (16)) are defined in terms of a bidimensional lattice with periods ω_1 and ω_2. Herein, we assume that $\omega_1 = \alpha > 0$ and $\omega_2 = re^{i\theta}$ where $r = |\omega_2|$ and θ the angle of inclination of the cell Y (see Fig. 1). These lattice sums S_{k+p} and E_{k+p}, as well as some formulas for their calculations, need to be determined in order to find the ${}_{pq}N_k$ local function as a solution of Eqs. (7)–(9), which can be written in terms of the $\wp(z)$ and $\zeta(z)$ functions.

3 Computation of Eisenstein–Rayleigh lattice sums S_{k+p} and E_{k+p}

3.1 Lattice sums S_{k+p} for a parallelogram periodic cell whose fiber is centered at the origin

In this section, the lattice sums S_{k+p} (Eq. 15) evaluation is carried out following Rayleigh's method [34] for a parallelogram periodic cell ($\omega_1 = \alpha$ and $\omega_2 = re^{i\theta}$) with a fiber centered at the origin on Y. These lattices sums are defined as a function of the principal periods ω_1 and ω_2 which depend on the angle θ of the unit cell, see Fig. 1.

The sum of order $k + p \geq 2$ can then be written for a parallelogram unit cell as follows:

$$S_{k+p}(1, \tau) = \sum_{s,t}{}' \frac{1}{(s\omega_1 + t\omega_2)^{k+p}} = \omega_1^{-(k+p)} \sum_{s,t}{}' \frac{1}{(s + it\tau)^{k+p}}, \tag{17}$$

such that, $\operatorname{Im}\tau > 0$ and the period ratio $\tau = -i\omega_2/\omega_1$.

Regarding the sum $\sum_{s,t}' \frac{1}{(s+it\tau)^{k+p}}$ in Eq. (17), it is convenient to analyze the following equation

$$\sin(\xi - it\tau\pi) = 0, \tag{18}$$

which leads to the lattice sums evaluation in a convenient way.

The zeroes of Eq. (18) are $\xi - it\tau\pi = 2k\pi$, $k \in \mathbb{Z}$. By means of Weierstrass factorization theorem, it follows that

$$\sin(\xi - it\tau\pi) = A\left(1 - \frac{\xi}{it\tau\pi}\right)\prod_{\mathrm{m}=1}^{\infty}\left(1 - \frac{\xi}{it\tau\pi + \mathrm{m}\pi}\right)\left(1 - \frac{\xi}{it\tau\pi - \mathrm{m}\pi}\right), \tag{19}$$

where m is a natural number and $\mathrm{A} = -\sin(it\tau\pi)$ when $\xi = 0$.

Next, Eq. (19) is divided by $\sin(i\pi t\tau)$; the logarithm properties and trigonometric identities are applied to get:

$$\ln\left[\cos\left(\xi\right)-\sin\left(\xi\right)\cot\left(i\pi t\tau\right)\right]=\ln\left(1-\frac{\xi}{i\pi t\tau}\right)+\sum_{\mathrm{m}=1}^{\infty}\left[\ln\left(1-\frac{\xi}{i\pi t\tau+\mathrm{m}\pi}\right)+\ln\left(1-\frac{\xi}{i\pi t\tau-\mathrm{m}\pi}\right)\right]. \tag{20}$$

An analogous expression to Eq. (20) is obtained by replacing t by -t. Then, the obtained formula is added to Eq. (20), and after the use of logarithm and trigonometric properties like

$$\cos^2\left(\xi\right)-\sin^2\left(\xi\right)\cot^2\left(i\pi t\tau\right)=1-\sin^2\left(\xi\right)/\sin^2\left(i\pi t\tau\right),$$

it leads to

$$\ln\left[1-\frac{\sin^2\left(\xi\right)}{\sin^2\left(it\tau\pi\right)}\right]=\sum_{s\in\mathbb{Z}}\ln\left[1-\frac{\xi^2}{\left(it\tau\pi+s\pi\right)^2}\right]. \tag{21}$$

Now, the left-hand and right-hand sides of Eq. (21) are expanded in Taylor power series of $\sin^2\left(\xi\right)/\sin^2\left(it\tau\pi\right)$ and $\xi^2/\left(it\tau\pi+s\pi\right)^2$, respectively.

Thus,

$$\sum_{\mathrm{m}=1}^{\infty}\frac{\sin^{2m}\left(\xi\right)}{m\sin^{2m}\left(it\tau\pi\right)}=\sum_{\mathrm{m}=1}^{\infty}\frac{\xi^{2m}}{m\,\pi^{2m}}\sum_{\forall s\in\mathbb{Z}}\frac{1}{\left(it\tau+s\right)^{2m}}. \tag{22}$$

Note that, on the right-hand side of Eq. (22), the sums of Eq. (17) appear where $2m=k+p$.

Subsequently, by developing the ξ power expansion for $\sin^{2m}\left(\xi\right)$ on the left-hand side of Eq. (22) around $\xi=0$ and by matching the ξ^n coefficients, it is obtained that

$$\xi^2:\quad\frac{\pi^2}{\sin^2\left(it\tau\pi\right)}=\sum_{\forall s\in\mathbb{Z}}\frac{1}{\left(it\tau+s\right)^2}, \tag{23}$$

$$\xi^4:\quad-\frac{2\pi^4}{3\sin^2\left(it\tau\pi\right)}+\frac{\pi^4}{\sin^4\left(it\tau\pi\right)}=\sum_{\forall s\in\mathbb{Z}}\frac{1}{\left(it\tau+s\right)^4}, \tag{24}$$

$$\xi^6:\quad\frac{2\pi^6}{15\sin^2\left(it\tau\pi\right)}-\frac{\pi^6}{\sin^4\left(it\tau\pi\right)}+\frac{\pi^6}{\sin^6\left(it\tau\pi\right)}=\sum_{\forall s\in\mathbb{Z}}\frac{1}{\left(it\tau+s\right)^6}, \tag{25}$$

and so on for the rest of ξ^n terms.

Now, in order to obtain the lattice sums S_{k+p} the case when s and t approach to zero in Eqs. (23)–(25) is considered. Therefore, from Eq. (23), we have that

$$\frac{\pi^2}{\sin^2\left(it\tau\pi\right)}=\sum_{-\infty}^{s=-1}\frac{1}{\left(it\tau+s\right)^2}+\frac{1}{\left(it\tau\right)^2}+\sum_{s=1}^{\infty}\frac{1}{\left(it\tau+s\right)^2}, \tag{26}$$

and the limit value of Eq. (26) when $t\to0$ has the form:

$$\lim_{t\to0}\left[\frac{\pi^2}{\sin^2\left(it\tau\pi\right)}-\frac{1}{\left(it\tau\right)^2}\right]=2\sum_{s=1}^{\infty}\frac{1}{s^2}. \tag{27}$$

Then, considering Eq. (17) for $k+p=2$ and combining it with Eq. (23), it is obtained that

$$\omega_1^2S_2=\sum_{t=-\infty}^{t=-1}\frac{\pi^2}{\sin^2\left(it\tau\pi\right)}+\left[\sum_{s=-\infty}^{s=+\infty}{}'\frac{1}{\left(s+it\tau\right)^2}\right]\Bigg|_{t=0}+\sum_{t=1}^{t=+\infty}\frac{\pi^2}{\sin^2\left(it\tau\pi\right)}. \tag{28}$$

Next, the term $\left(it\tau\right)^{-2}$ is added and subtracted in Eq. (28); after conveniently grouping and replacing Eqs. (23) and (27), it can be written S_2 as:

$$S_2=\frac{2}{\omega_1^2}\sum_{t=1}^{\infty}\frac{\pi^2}{\sin^2\left(it\tau\pi\right)}+\frac{2}{\omega_1^2}\sum_{s=1}^{\infty}\frac{1}{s^2}. \tag{29}$$

Analogously, the expression of the lattice sum S_4, S_6, and so on is found as follows:

$$S_4 = \frac{2\pi^4}{\omega_1^4}\sum_{t=1}^{\infty}\left[-\frac{2}{3\sin^2(it\tau\pi)} + \frac{1}{\sin^4(it\tau\pi)}\right] + \frac{2}{\omega_1^4}\sum_{s=1}^{\infty}\frac{1}{s^4}, \tag{30}$$

$$S_6 = \frac{2\pi^6}{\omega_1^6}\sum_{t=1}^{\infty}\left[\frac{2}{15\sin^2(it\tau\pi)} + \sum_{m=2}^{3}\frac{(-1)^{m+1}}{\sin^{2m}(it\tau\pi)}\right] + \frac{2}{\omega_1^6}\sum_{s=1}^{\infty}\frac{1}{s^6}. \tag{31}$$

In order to find the second sums of Eqs. (29)–(31), the Zeta Riemann function $\zeta(n) = \sum_{s=1}^{\infty} s^{-n}$ ($n = 2$, 4, and 6) is also computed. For that, the formula $\zeta\,(2\mathrm{p}) = (-1)^{\mathrm{p}-1}\,2^{2\mathrm{p}-1}\pi^{2\mathrm{p}}B_{2\mathrm{p}}/\,(2\mathrm{p})!$ is used, where $B_{2\mathrm{p}}$ is the Bernoulli numbers and p is a natural number. Therefore, $\zeta\,(2) = \pi^2/6$, $\zeta\,(4) = \pi^4/90$ and $\zeta\,(6) = \pi^6/945$. Thus, the lattice sums can be computed as follows:

$$S_2 = \frac{2\pi^2}{\omega_1^2}\left[\frac{1}{6} + \sum_{t=1}^{\infty}\frac{1}{\sin^2(it\tau\pi)}\right], \tag{32}$$

$$S_4 = \frac{2\pi^4}{\omega_1^4}\left[\frac{1}{90} + \sum_{t=1}^{\infty}\left(\frac{1}{\sin^4(it\tau\pi)} - \frac{2}{3\sin^2(it\tau\pi)}\right)\right], \tag{33}$$

$$S_6 = \frac{2\pi^6}{\omega_1^6}\left[\frac{1}{945} + \sum_{t=1}^{\infty}\left(\frac{2}{15\sin^2(it\tau\pi)} + \sum_{m=2}^{3}\frac{(-1)^{m+1}}{\sin^{2m}(it\tau\pi)}\right)\right]. \tag{34}$$

The lattice sums expressions (Eqs. (32)–(34)) respond to any 2D lattice of a parallelogram periodic cell with a fiber centered at origin as function of the period ratio $\tau = -i\omega_2/\omega_1$. For example, $\tau = 1$ for square periodic cell ($\omega_1 = \alpha$, $\omega_2 = \alpha i$ and $\alpha \neq 0$) and $\tau = r/\alpha$ for rectangular periodic cell ($\omega_1 = \alpha$, $\omega_2 = ri$, $r \neq \alpha$). Details of the sums convergences analysis can be found in Ref. [34]. Representations of Eqs. (32)–(34) in terms of hyperbolic function sum are reported in Refs. [37,47]. Both representations can be transformed into each other applying the appropriate trigonometric identities. Also, the expressions of the sums S_2, S_4 and S_6 in terms of powers of exponential functions $e^{i\pi\tau}$ are given in Ref. [43].

Then, the remaining S_{k+p} are calculated based on the power series of the Weierstrass function $\wp\,(z)$, see, for instance, Ref. [55,56]. The expression $(z - \beta_{st})^{-2} - \beta_{st}^{-2}$ of $\wp\,(z)$ with β_{st} non-null is developed in Taylor expansion of z for this purpose, and therefore,

$$\wp\,(z) = z^{-2} + \sum_{k=2}^{\infty} c_k z^{2k-2}, \tag{35}$$

and $\zeta\,(z) = \frac{1}{z} - \sum_{k=2}^{\infty}\frac{c_k}{(2k-1)}z^{2k-1}$, where $c_k = (2k-1)\,S_{2k}$ (herein, S_{2k} denotes S_{k+p}) satisfies the recursive formula:

$$c_k = \frac{3}{(2k+1)\,(k-3)}\sum_{m=2}^{k-2} c_m c_{k-m}, \ \text{ for } k \geq 4 \tag{36}$$

and thus, $S_{2k} = c_k/(2k-1)$, see Ref. [28].

From Eq. (36) an alternative recursion formula for the lattice higher-order sums is obtained as follows:

$$S_{2k} = \frac{3}{(2k+1)\,(2k-1)\,(k-3)}\sum_{m=2}^{k-2}(2m-1)\,(2k-2m-1)\,S_{2m}S_{2k-2m}, \ \text{ for } k \geq 4. \tag{37}$$

Equation (37) yields the following lattice sums

$S_8 = \frac{3}{7}S_4^2$, $S_{10} = \frac{5}{11}S_4S_6$, $S_{12} = \frac{1}{143}\left(18S_4^3 + 25S_6^2\right)$, $S_{14} = \frac{30}{143}S_4^2S_6$, $S_{16} = \frac{1}{2431}\left(99S_4^4 + 300S_4S_6^2\right)$, and so on, as a combination of S_4 and S_6, see, for instance, Ref. [47,57]. In case of square periodic cell ($\tau = 1$), it is important to mention that the lattice sums $S_6 = S_{10} = S_{14} = \cdots = 0$, and hence, $S_8 = \frac{3}{7}S_4^2$, $S_{12} = \frac{18}{143}S_4^3$, $S_{16} = \frac{99}{2431}S_4^4$, and so on. These results are also stated in Ref. [34,47].

3.2 Lattice sums E_{k+p} for a parallelogram periodic cell with a fiber not centered at the origin

For some spatial fiber distribution of multiphase periodic composites, more than one fiber may be associated to the unit cell. One of them is conveniently positioned at the coordinate origin as it always done for one fiber unit cell. The second fiber and any other one cannot be positioned in the same coordinate component. Therefore, the necessity of lattice sum arises for periodic composite with a fiber not centered at the origin. As follows, the Eisenstein lattice sums at any point $z = z_1$ (Eq. 16) inside of the periodic parallelogram cell Y need to be calculated.

Let $\frac{z-z_1}{\omega_1} = a + ib \in \mathbb{C}$, the lattice sums E_{k+p} (Eq. 16) corresponding to a parallelogram cell Y are rewritten as follows:

$$E_{k+p} = \omega_1^{-(k+p)} \sum_{s,t} \frac{1}{(a + ib - s - it\tau)^{k+p}}, \text{ with } \tau = -i\omega_2/\omega_1. \tag{38}$$

Regarding Eq. (38), there are different approaches for determine the Eisenstein lattice sums. In fact, a direct inference of the above procedure can be generalized. It is convenient to analyze more general form of Eq. (18), as follows:

$$\sin(\xi - a\pi - ib\pi - it\pi) = 0. \tag{39}$$

Then, by developing the same procedure previously shown for the calculation of the S_{k+p}, we can obtain:

$$\begin{aligned} E_2 = {} & \frac{1}{\omega_1^2(a+ib)^2} + \frac{\pi^2}{\omega_1^2}\sum_{t=1}^{+\infty}\left[\frac{1}{\sin^2(a\pi + i\pi \mathrm{b} - i\mathrm{t}\tau\pi)} + \frac{1}{\sin^2(a\pi + i\pi \mathrm{b} + i\mathrm{t}\tau\pi)}\right] \\ & + \frac{1}{\omega_1^2}\sum_{s=1}^{\infty}\frac{1}{(a + i\mathrm{b} + s)^2} + \frac{1}{\omega_1^2}\sum_{s=1}^{\infty}\frac{1}{(a + i\mathrm{b} - s)^2}, \end{aligned} \tag{40}$$

$$\begin{aligned} E_4 = {} & \frac{1}{\omega_1^4(a+ib)^4} \\ & + \frac{\pi^4}{\omega_1^4}\sum_{t=1}^{+\infty}\left[-\frac{2}{3\sin^2(a\pi + i\pi \mathrm{b} - i\mathrm{t}\tau\pi)} + \frac{1}{\sin^4(a\pi + i\pi \mathrm{b} - i\mathrm{t}\tau\pi)}\right] + \frac{1}{\omega_1^4}\sum_{s=1}^{\infty}\frac{1}{(a + i\mathrm{b} + s)^4} \\ & + \frac{\pi^4}{\omega_1^4}\sum_{t=1}^{+\infty}\left[-\frac{2}{3\sin^2(a\pi + i\pi \mathrm{b} + i\pi \mathrm{t}\tau)} + \frac{1}{\sin^4(a\pi + i\pi \mathrm{b} + i\pi \mathrm{t}\tau)}\right] + \frac{1}{\omega_1^4}\sum_{s=1}^{\infty}\frac{1}{(a + i\mathrm{b} - s)^4}, \end{aligned} \tag{41}$$

$$\begin{aligned} E_6 = {} & \frac{1}{\omega_1^6(a+ib)^6} \\ & + \frac{\pi^6}{\omega_1^6}\sum_{t=1}^{+\infty}\left[\frac{2}{15\sin^2(a\pi + i\pi \mathrm{b} + i\mathrm{t}\tau\pi)} + \sum_{m=2}^{3}\frac{(-1)^{m+1}}{\sin^{2m}(a\pi + i\pi \mathrm{b} + i\mathrm{t}\tau\pi)}\right] + \frac{1}{\omega_1^6}\sum_{s=1}^{\infty}\frac{1}{(a + i\mathrm{b} + s)^6} \\ & + \frac{\pi^6}{\omega_1^6}\sum_{t=1}^{+\infty}\left[\frac{2}{15\sin^2(a\pi + i\pi \mathrm{b} - i\mathrm{t}\tau\pi)} + \sum_{m=2}^{3}\frac{(-1)^{m+1}}{\sin^{2m}(a\pi + i\pi \mathrm{b} - i\mathrm{t}\tau\pi)}\right] + \frac{1}{\omega_1^6}\sum_{s=1}^{\infty}\frac{1}{(a + i\mathrm{b} - s)^6}. \end{aligned} \tag{42}$$

The remaining E_{k+p} are calculated based on the same procedure.

Table 1 Lattice sum values S_{k+p} for different rectangular cells with periods $\omega_1 = 1$, $\omega_2 = ri$ and period ratio $|\tau|$ equal to 0.5, 0.7, 0.9, 1 and 1.1

S_{k+p}	Period ratio $\lvert\tau\rvert$				
	$\lvert\tau\rvert = 0.5$	$\lvert\tau\rvert = 0.7$	$\lvert\tau\rvert = 0.9$	$\lvert\tau\rvert = 1$	$\lvert\tau\rvert = 1.1$
S_2	−0.5920005108408	2.2823394084011	3.0105684953659	3.1415926535898	3.2109713046499
S_4	34.663332023693	9.2894343371550	4.0410983423536	3.1512120021539	2.6868729667528
S_6	−129.99100840070	−16.188098309315	−1.9805024643618	0	0.9792045710845
S_8	514.94853727919	36.982967273277	6.9987753482455	4.2557730353652	3.0939798597715
S_{10}	−2048.1461292219	−68.353761948997	−3.6379114662545	0	1.1959083140762
S_{12}	8196.7447956950	146.71677417544	8.9925511016237	3.9388490128279	2.6092484985071
S_{14}	−32767.185835505	−293.06205384126	−6.7851498442662	0	1.4830401783721
S_{16}	131076.30157297	603.66650969680	12.816531763928	4.0156950330250	2.4403854774905
S_{18}	−524288.25477502	−1226.1941945545	−11.309394623311	0	1.6378840498569
S_{20}	2097155.5721637	2508.5806704183	18.445283742342	3.9960967531763	2.2964539312937

Table 2 As in Table 1 but for rectangular cells with period ratio $|\tau|$ equal to 1.5, 1.9, 2, 4 and 6

S_{k+p}	Period ratio $\lvert\tau\rvert$				
	$\lvert\tau\rvert = 1.5$	$\lvert\tau\rvert = 2$	$\lvert\tau\rvert = 4$	$\lvert\tau\rvert = 6$	$\lvert\tau\rvert = 8$
S_2	3.2834948124219	3.28959278129999	3.2898681327362	3.2898681336965	3.2898681336964
S_4	2.2066015468913	2.1664582514808	2.1646464737404	2.1646464674223	2.1646464674223
S_6	1.9517097194760	2.0311095062610	2.0346861114974	2.0346861239689	2.0346861239689
S_8	2.0867530228898	2.0115177237468	2.0081547241186	2.0081547123959	2.0081547123959
S_{10}	1.9575662209448	2.0001427043183	2.0019891438279	2.0019891502556	2.0019891502556
S_{12}	2.0183484864025	2.0011583973865	2.0004921754135	2.0004921731066	2.0004921731066
S_{14}	1.9936470698210	1.9999503073429	2.0001224956863	2.0001224962701	2.0001224962701
S_{16}	2.0027530857222	2.0000656367946	2.0000305646286	2.0000305645188	2.0000305645188
S_{18}	1.9986940518661	2.0000009718896	2.0000076345706	2.0000076345865	2.0000076345865
S_{20}	2.0006244668488	2.0000034066807	2.0000019079259	2.0000019079241	2.0000019079241

An alternative method for computing the Eisenstein lattice sums (E_{k+p} (38)) is the suitable representation given by Rogosin [43] due to Weil [57] in the form of power series is implemented, such as:

$$E_{k+p} = \frac{1}{(a+ib)^{k+p}} + (-1)^{k+p} \sum_{m=1}^{\infty} \frac{(2m-1)!}{(k+p-1)!(2m-k-p)!} S_{2m} (a+ib)^{2m-(k+p)}, \tag{43}$$

for $k + p \geq 2$, where $S_{2m} (m \geq 1)$ are the corresponding lattice sums S_{k+p} for a parallelogram periodic cell, see Eqs. (32)–(34) and (37). Construction of Eisenstein summation, convergence proof and properties are well established by Weil [57]. Generalized Eisenstein lattice sums E_{k+p} formula and some properties are defined in [43]. Equation (43) is based on the close relationship between the Eisenstein series and the Weierstrass elliptic functions. Recently, an equivalent representation of the Eisenstein lattice sums E_{k+p} as a function of Weierstrass elliptic $\wp$-function and its derivates is formulated in [32]. In his work, it is proposed that the Weierstrass elliptic functions values are calculated via Mathematica software (Wolfram Research, Champaign, IL).

In summary, the expressions here developed to compute the lattice sums S_{k+p} [Eqs. (32)–(34) and (37)] are convergent and only few terms of the sums $\sum_{t=1}^{+\infty} \frac{1}{\sin^{\mathrm{k+p}}(it\tau\pi)}$ are required to obtain good precision rounded-off to 14D (accuracy digits). Rayleigh's methodology becomes cumbersome to calculate the Eisenstein lattice sum E_{k+p}. However, the proposed alternative method to compute the sums E_{k+p} is easy to implement and rapidly converges.

4 Numerical results

In this section, the numerical computations of the Eisenstein–Rayleigh lattice sums, S_{k+p} and E_{k+p}, are tabulated for a FRC with square, rectangular or parallelogram periodic cell. The lattice sums S_2, S_4 and S_6

Table 3 Lattice sum values for different parallelogram unit cells with periods $\omega_1 = 1, \omega_2 = e^{i\theta}$ considering θ equal to 10°(170°), 20°(160°), 30°(150°), 40°(140°) and 45°(135°)

S_{k+p}	Principal angle θ°				
	10°(170°)	20°(160°)	30°(150°)	40°(140°)	45°(135°)
S_2	−70.721071334723 ±15.660089765079i	−7.8140539240382 ±6.1872961094248i	1.0894973681625 ±2.9985771296784i	3.2223716658098 ±1.3971670738117i	3.5648833303306 ±0.8779996078278i
S_4	2203.2753592696 ∓801.92664866631i	113.98248849401 ∓95.642664055996i	15.045542089697 ∓26.059643326772i	1.6434502330263 ∓9.3204694280084i	∓5.5422300524424i
S_6	−62816.253571938 ±36266.980909242i	−579.78914112903 ±1004.2242501122i	±106.19578899462i	10.818316750821 ±18.737874264795i	8.9604887255531 ±8.9604887255531i
S_8	1804858.2681100 ∓1514455.9070984i	1647.6379266686 ∓9344.2190188280i	−194.03000294816 ∓336.06982329895i	−36.072952152859 ∓13.12948084575i	−13.164134551798
S_{10}	−49690020.544949 ±59218260.500523i	13618.578855759 ±77234.798673701i	1257.9201745477 ±726.26055139418i	87.465977007259 ∓31.835012141655i	22.573222681514 ∓22.573222681514i
S_{12}	1271144178.81290 ∓2201686301.4494i	−324865.35556693 ∓562683.30146085i	−5401.2502431904 ∓3.251656708(−12)i	−94.275482356322 ±163.28992534921i	±49.501970065649i
S_{14}	−28611736931.656 ±78610101151.099i	4125794.4972519 ±3461952.6409574i	17470.237783049 ∓10086.446486850i	−70.602127897900 ∓400.40456437369i	−57.741227596599 ∓57.741227596599i
S_{16}	478069237318.08 ∓2711265374120.6i	−41958388.748949 ∓15271604.582387i	−37633.564056908 ±65183.245016462i	669.14100367519 ±561.47596938945i	148.25104238393
S_{18}	0.2173713235294 ±90607381889123i	370192483.55066 ∓6.9085104916(−7)i	2.334596002(−10) ∓280904.99449578i	−1856.2149569467 ±2.400798514(−12)i	−172.12811215039 ±172.12811215039i
S_{20}	−51782207430978 ∓29367149158297i	−2884109282.3785 ±1049729931.1566i	524175.51553214 ±907898.62498527i	3047.7897200719 ∓2557.3992300182i	−2.2987666431(−13) ∓420.37634672695i

(n) at the end of the number represents the factor 10^n

Table 4 As in Table 3 but for parallelogram unit cells with θ equal to 50°(130°), 60°(120°), 70°(110°), 75°(105°) and 80°(100°)

S_{k+p}	Principal angle θ°				
	50°(130°)	60°(120°)	70°(110°)	75°(105°)	80°(100°)
S_2	3.6932285542562 ±0.4860321476729i	3.6275987284684	3.4082755960930 ∓0.1787578154579i	3.3012429523105 ∓0.1822245070218i	3.2155753348186 ∓0.1447228924140i
S_4	−0.5290569122952 ∓3.0004308482430i	0	1.3764654366096 ±1.1549916401874i	2.0732516774552 ±1.1969924140766i	2.6458145492337 ±0.9629977413095i
S_6	7.6088013435543 ±4.3929435039114i	5.8630316934254	3.6598374207887 ∓2.1130081200826i	2.3455048403593 ∓2.3455048403593i	1.1464333070493 ∓1.9856807352986i
S_8	−3.7382931679889 ±1.3606274401087i	0	0.2402791754049 ±1.3626909191066i	1.2281064337345 ±2.1271427403304i	2.6027014196441 ±2.1839258012879i
S_{10}	4.1614701175618 ∓11.433545179736i	0	3.3991574671226 ±0.5993631731304i	3.4865333390201 ∓0.9342137925746i	2.2479345393507 ∓1.8862410428798i
S_{12}	8.5274660391398 ±14.770004439608i	6.0096399716977	1.1959959364450 ∓2.0715257275687i	∓0.1965309199381i	0.9452924457808 ±1.6372945441035i
S_{14}	−16.849484396800 ∓2.9710187101821i	0	1.8399522981628 ±2.1927697615375i	3.8523267306759 ±1.0322278364655i	3.5834140494450 ∓1.3042560510493i
S_{16}	24.920796185129 ∓20.911030887587i	0	3.3223934228808 ∓1.2092523124504i	0.9564733963214 ∓1.6566605185167i	0.1272384052495 ±0.7216048544489i
S_{18}	±41.250108473341i	5.9997183563705	∓0.1687033431809i	1.9594308960584 ±1.9594308960584i	3.9791922542289
S_{20}	−41.883373435003 ∓35.144323201771i	0	3.6528485247371 ±1.3295281332875i	3.0339788853664 ∓1.7516685261819i	0.1229676598607 ∓0.6973842537691i

for a periodic cell with a fiber centered at the coordinate origin are computed by means of Eqs. (32)–(34). For calculating S_{2k} when $k \geq 4$, the recurrent relation (Eq. 37) is used. For periodic cell with a fiber not centered at the coordinate origin, the Eisenstein lattice sums E_{k+p} are determined using Eq. (43).

a) Lattice sum S_{k+p} values for a rectangular periodic cell with a fiber center at the coordinate system origin.

In Tables 1 and 2, the lattice sum values (S_2, $S_4, \ldots,$ S_{20}) rounded off to 14D (accuracy digits) are reported for a periodic rectangular unit cell with different period ratio values $|\tau|$ between 0.5 and 8, such as $\tau = -i\omega_2/\omega_1$, $\omega_1 = 1$, $\omega_2 = ri$ with $r > 0$ and $|\tau| = r$. The case of a square periodic unit cell is defined when $|\tau| = 1$. From Tables 1 and 2, it can be seen that the values of S_6, S_{10}, S_{12} and S_{14} sum are negative when $0.5 \leq |\tau| < 1$ and positive when $|\tau| \geq 1$. The remaining ones always are positive. In addition, when $|\tau| > 6$, the numerical values of the lattice sums become equal to those obtained when $|\tau| = 6$ with more

Table 5 Eisenstein lattice sum values E_{k+p} for different cells with a fiber centered at $(0.5,\ 0.5)$, such as $\omega_1 = 1$, $\omega_2 = ri$ and period ratio $|\tau|$ equal to 0.9, 1.1 and 2 (rectangular cell) and $|\tau| = 1$ (square cell)

E_{k+p}	Period ratio $\|\tau\|$			
	$\|\tau\| = 0.9$	$\|\tau\| = 1$	$\|\tau\| = 1.1$	$\|\tau\| = 2$
E_1	−3.3529696258591i	−3.1415926535898i	−3.0227817691577i	−2.881825103941i
E_2	4.3213841547184	3.1415926535898	2.4397964938551	1.5707963267949
E_3	2.8084062553741i	0	−1.9105115904585i	−4.5067832278256i
E_4	−18.487254018964	−15.756060010769	−12.839654244959	−7.8780300053847
E_5	9.4146912488(−14) +3.6813028973678i	−1.8207657604(−14) +1.9095836024(−14)i	1.4733384142931i	7.7462430332096i
E_6	−17.69488751798 −2.0072832285(−13)i	2.7533531011(−14)i	4.480948944906 −1.0658141036(−14)i	4.9639392322(−14)
E_7	−1.9877433033(−12) −29.221628105051i	8.5265128291(−14) +8.3488771452(−14)i	−1.4210854715(−14) +14.263704362333i	−4.6185277824(−14) +15.977058073459i
E_8	76.53263396019 −1.9791294974(−12)i	63.836595530477	42.691194928516 +1.3408990231(−13)i	31.918297765239 −5.5227413236(−13)i
E_9	−1.3859136061(−11) −55.123411272099i	3.2525093729(−12) −4.6096459982(−12)i	4.2810199829(1) −13.521920569148i	1.8864909634(−12) −32.038195898431i
E_{10}	154.41828430542 −2.2348345396(−10)i	−1.9707810679e(−14) +2.1685764295(−11)i	−18.66234011688 +1.6342482922(−13)i	−2.3406465709(−14) +3.6166625250(−12)i

Table 6 Eisenstein lattice sum values E_{k+p} for two different cells with a fiber centered at the points $(0.1,\ 0.1)$ and $(0.5,\ 0.75)$

E_{k+p}	Square periodic cell ($\|\tau\| = 1$)		Rectangular periodic cell with $\|\tau\| = 2$	
	(0.1, 0.1)	(0.5, 0.75)	(0.1, 0.1)	(0.5, 0.75)
E_1	4.6921397552868 −5.3204582860048i	−3.05311331772(−14) −4.1693430802293i	4.6754532421897 −5.3332093736681i	−3.0531133177(−14) −4.1693430802293i
E_2	3.1415926535898 −49.81116546459i	5.9893878632418 −1.7534418362(−11)i	3.2855334408299 −49.870125079501i	5.9893878632418 −1.7534418362(−11)i
E_3	−250.94179221479 −250.94179221479i	3.0982647559(−09) +10.560049969354i	−250.60768492433 −250.68881419613i	3.0982647559(−09) +10.560049969354i
E_4	−2496.9082649516	−7.6461227010079 +2.4829522882(−07)i	−2497.8616502243 +0.4048796339699i	−7.6461227010079 +2.482952288(−07)i
E_5	−12499.703133992 +12499.703133992i	−5.8631649682(−06) +30.072831361188i	−12500.865218075 +12498.85422431i	−5.8631649682(−06) +30.072831361188i
E_6	125001.77290522i	−57.66884328667 +0.0007111763363i	1.930713352707 +125000.83746035i	−57.66884328667 +0.0007111763363i
E_7	624997.09342792 +624997.09342792i	−0.0861806864415 −14.130040958243i	624998.96204553 +624998.29547283i	−0.0861806864415 −14.130040958243i
E_8	6250003.7399667	−177.15829539363 −4.9013487520216i	6250001.7494176 +1.4127715993652i	−177.15829539363 −4.9013487520216i
E_9	31250001.279244 −31250001.279244i	168.86802446861 −217.32175501683i	31249998.952188 −31250002.34808i	68.86802446861 −217.32175501683i
E_{10}	−312499995.82688i	−6666.1624713214 +2945.1966114423i	1.4358986015529 −312499997.87822i	−6666.1624713214 +2945.1966114423i

than 15D accuracy. This pattern is also reported in Table 1 of Ref. [37] for the S_4 and S_6 sums, which are given for period ratios from 1 to infinity (as an infinite periodic rectangular cell). In Ling [40], calculations of the S_{k+p} lattice values are determined using the Weierstrass elliptic function $\wp(z)$ and its invariants through the differential equation $\left[\wp'(z)\right]^2 = 4\wp^3(z) - 60S_4\wp(z) - 140S_6$ and relate equations, see, for instance, Ref. [55,56]. Comparisons of herein reported S_{k+p} in Tables 1 and 2 with numerical values given in Table 1 of Ling [40] show a good accuracy with more than 15 significant digits for rectangular periodic cells with $|\tau|$ equal to 1, 1.5, 2, 4, and 6. In addition, validations with Table 1 of Huang [36] and Table 2 of Movchan [41] for square periodic cell confirm good agreements. A numerical sensitivity analysis of the lattice sums S_{k+p} is developed in Appendix A.

b) Lattice sum values for a parallelogram-like periodic cell with a fiber centered at the origin.

Tables 3 and 4 show the lattice sum $(S_2, S_4, \ldots, S_{20})$ with the same accuracy digits like in Tables 1 and 2. Different periodic parallelogram unit cells, such as $\omega_1 = 1$, $\omega_2 = e^{i\theta}$ with $\theta = 10°, 20°, 30°, 40°, 45°, 50°, 60°, 70°, 75°$ and $80°$, are considered. In addition, the corresponding lattice S_{k+p}

Table 7 Eisenstein lattice sum values E_{k+p} for different parallelogram periodic cells with a fiber not centered at origin

E_{k+p}	Parallelogram periodic cell with $\theta = 30°$		Parallelogram periodic cell with $\theta = 45°$	
	(0.1, 0.1)	(0.3, 0.3)	(0.1, 0.1)	(0.4, 0.4)
E_2	2.636054170888 −46.299351553886i	10.102065677404 −3.2846224150193i	3.8795269669671 −49.13921663826i	5.2651876212043 −5.637024372172i
E_3	−260.14059748974 −244.9977378253i	−9.7871914911815 +3.0094760349739i	−251.31526656099 −248.34713210758i	5.7838420020419 +4.1290262804492i
E_4	−2503.1216449943 −22.185877297831i	−33.479919438227 +17.042686439489i	−2501.6229203898 −3.764047365997i	−39.554502778408 +5.5561038055352i
E_5	−12480.203217659 +12445.489704663	−69.298593417175 +88.61798546149i	−12500.706960134 +12491.94918873i	36.734996604983 −30.661268238055
E_6	80.733006165107 +125005.72669426i	−82.101608236755 +194.81217957384i	7.9939296862416 +125004.55870927i	−12.072336649465 +179.39266925835i
E_7	625131.05062393 +625216.68271936i	138.72936734259 +333.1027846571i	625008.44682638 +625002.53450649i	−205.95026609194 −195.29672084858i
E_8	6249834.3975995 +394.48040077835i	539.99312744507 −136.23913140407i	6250002.4379098 +10.501699855019i	877.44383274042 −15.1333250199i
E_9	31248938.675266 −31250040.008732i	1141.073006159 −2090.3668578129i	31249975.064456 −31249988.855107i	−1186.8853219427 +1176.3677538897i
E_{10}	−1335.3292231479 −312501738.07563i	−791.07645035564 −6750.8916286593i	−15.919709490031 −312500011.33408i	14.817815564637 −4509.9946558579i
E_{k+p}	Parallelogram periodic cell $\theta = 60°$		Parallelogram periodic cell $\theta = 75°$	
	(0.1, 0.1)	(0.5, 0.5)	(0.1, 0.1)	(0.5, 0.5)
E_2	3.6158726650842 −49.999999788461i	−3.3131622532022	3.2248565420684 −50.053208516798i	1.6720672045178 +2.1203605876922i
E_3	−249.88274465472 −250.11726592225i	−23.228677538281i	−250.26370652566 −251.07194759216i	−6.6009767582429 −3.4739817705185i
E_4	−2499.9998413455 +1.1726063334629i	48.174163004682 −4.9054860358(−14)i	−2497.475469607 +1.6339688171064i	−13.01394288848 −13.487593657457i
E_5	−12502.9331023 +12497.07007079i	1.4832579609(−13) +161.22469871351i	−12502.088337517 +12500.075791157i	18.75328973994 −9.5395839517211i
E_6	5.8630293173449 +124999.97778837i	−416.4477946155 +5.186961971(−13)i	1.2764656198932 +124998.21760516i	43.956737463734 +13.550107734193i
E_7	625000.11108191 +625000.11103438i	−1.8989254613(−12) −1119.0220981123i	625001.05484855 +624996.90893589i	19.994768148734 +104.03397675872i
E_8	6249999.2067276 +0.0003733840704i	3134.6280134422 −5.1901611237(−12)i	6250001.915764 +4.6089259372612i	−104.34266980453 +111.88628353539i
E_9	31250001.980847 −31250001.985514i	1.0350831303(−11) +8447.8172792219i	31249996.105285 −31250002.098672i	−304.86505347155 −168.1306483165i
E_{10}	0.0233365039036 −312499993.3894i	−23168.937030255 +5.4690474372(−11)i	2.5427532727064 −312500001.25923i	−38.434394046035 −629.34693717973i

values associate to the supplementary angle $180° - \theta$ are given. It is important to notice that for two supplementary angles, the corresponding S_{k+p} values are complex conjugate numbers, where the upper (lower) sing of imaginary part corresponds to θ or $(180° - \theta)$ angle. To illustrate the accuracy and validate the present model, the S_4 and S_6 values are compared with the result reported in Table 1 of Ling [39] and a exactly coincidence is obtained for more than 15D.

c) Eisenstein lattice sum E_{k+p} values for different periodic cells with a fiber centered at the point (a, b).

In Tables 5, 6 and 7, the values of the Eisenstein lattice sums (E_{k+p}) are reported for different periodic cells with a fiber centered at the point (a, b). Here, numerical computations are carried out by mean of Eq. (43) and the corresponding lattice sums S_{k+p} using Eqs. (32)–(34) and (37) for parallelogram periodic cell. It is important to note that good coincidences are obtained when the values of E_2, E_4 and E_6 are compared by the two different approaches: the first one using Eqs. (40–42) following the Rayleigh methodology herein developed and the other one by Eq. (43) taken from [43] combining with the lattice sums S_{k+p} computed by Eqs. (32)–(34) and (37). In addition, the center of the fiber depends on the limit of percolation for each cell configuration.

d) Eisenstein lattice sum E_{k+p} values for four parallelogram periodic cells with a fiber centered at the point (a, b).

The lattice sum values S_{k+p} reported in Tables 1, 2, 3 and 4 have been applied to calculate the effective elastic properties of multiphase FRCs with square, rectangular or parallelogram periodic cells under different interface conditions as reported in Refs. [9,13,26,53,58,59]. In addition, they are used to solve transport problems [23,42,44,45] and for coupled field problems [22,24,60]. On the other hand, the E_{k+p} sums have been used to compute the effective conductivities on two-phase FRC in Refs. [32,33]. Former besides applying theory to a unit cell of a single inclusion (centered at the origin) calculated conductivities for a unit cell with two inclusions (one centered and one not at the origin) [32]. The latter use generalized Eisenstein–Rayleigh sums to find the effective conductivity for three inclusions [33].

5 Conclusions

In this work, Rayleigh's methodology for lattice sums calculation is extended for fiber-reinforced composites with parallelogram periodic cells whose fiber is centered at the origin. New lattice sums are obtained which are simple analytical formulas easy to implement numerically. Also, the Eisenstein lattice sums for parallelogram periodic cells with a fiber not centered at the origin are implemented using two different approaches: the first one follows Rayleigh's methodology, and the other one combines Rogosin's Eisenstein series representation in the form of a power series [43] with Rayleigh's procedure applied to the sum values S_{k+p}. Comparisons with lattice sum values reported in the literature by other methods were performed when possible. Good agreement is attained for all the performed comparisons. Lattice sums numerical values and easy-to-use formulae are reported for a wide variety of cases.

Acknowledgements The author YEA gratefully acknowledges the Program of Postdoctoral Scholarships of DGAPA from UNAM, México. HCM is grateful to the support of the CONACYT Basic science grant A1-S-9232. FJS thanks the funding of DGAPA, UNAM. This work was supported by the project PAPIIT-DGAPA-UNAM IA100919. The author is also grateful to M. Sc. Suset Rodríguez Alemán for computational assistance. Thanks to the Department of Mathematics and Mechanics, IIMAS-UNAM, for its support and Ramiro Chávez Tovar and Ana Pérez Arteaga for computational assistance.

Declarations

Conflict of interest The authors declare that they have no conflict of interest.

Appendix A

The numerical sensitivity of the lattice sums S_{k+p} when $|\tau|$ increases is performed through an analysis of the numerical values of the infinite series $G^{-n}(\tau) = \sum_{t=1}^{+\infty} \frac{1}{\sin^n(it\tau\pi)}$, $\quad n = k + p, (k + p = 2, 4, 6, \ldots)$ which are parts of the S_{k+p} expressions.

In Table 8, an analysis of the numerical sensitivity of the $G^{-n}(\tau)$ is reported for different $|\tau|$ values and numbers of terms N of the sums. As it is observed, for a fixed $|\tau|$ only a few terms N are needed to obtain the sum value. Also, as $|\tau|$ increases, the required number of terms is getting lower and the sums tend to cero. Then, $|\tau| \to \infty$ implies $G_N^{-n}(\tau) = \sum_{t=1}^{N} \frac{1}{\sin^{\mathrm{k+p}}(it\tau\pi)} \to 0$ for all values of $N \geq 1$. Therefore, from Eqs. (32)–(34), it is observed that the lattice sums S_{k+p} is a linear combination of the sums $G^{-n}(\tau)$ to any period ratio$|\tau|$; thus, when $|\tau| \to \infty$ implies that $S_2 = \frac{2\pi^2}{\omega_1^2}\left[\frac{1}{6} + \sum_{t=1}^{\infty} \frac{1}{\sin^2(it\tau\pi)}\right] \to \frac{\pi^2}{3\omega_1^2}$, $S_4 = \frac{2\pi^4}{\omega_1^4}\left[\frac{1}{90} + \sum_{t=1}^{\infty}\left(\frac{1}{\sin^4(it\tau\pi)} - \frac{2}{3\sin^2(it\tau\pi)}\right)\right] \to \frac{\pi^4}{45\omega_1^4}$, and $S_6 = \frac{2\pi^6}{\omega_1^6}\left[\frac{1}{945} + \sum_{t=1}^{\infty}\left(\frac{2}{15\sin^2(it\tau\pi)} + \sum_{m=2}^{3} \frac{(-1)^{m+1}}{\sin^{2m}(it\tau\pi)}\right)\right] \to \frac{2\pi^6}{945\omega_1^6}$.

For $\omega_1 = 1$, we have that $S_2 \to \frac{\pi^2}{3} \approx 3.289868133696453$, $S_4 \to \frac{\pi^4}{45} \approx 2.164646467422276$, and $S_6 \to \frac{2\pi^6}{945} \approx 2.034686123968898$, which are the values reported in Table 2 when $|\tau| \geq 6$. The remaining values of S_{k+p} can be computed by the recursive formula Eq. (37). For these cases, a numerical precision of 1×10^{-8} is considered.

Table 8 Numerical values of the series $G^{-n}(\tau)$ for different period ratios $|\tau|$ and number of terms N of the sums. The $(\times 10^n)$ under the $|\tau|$ is a factor that multiplies the sum value

N	$G_N^{-2}(\tau)$				
	$\tau = 1$ $(\times 10^{-3})$	$\tau = 1.1$ $(\times 10^{-3})$	$\tau = 2$ $(\times 10^{-5})$	$\tau = 4$ $(\times 10^{-11})$	$\tau = 6$ $(\times 10^{-16})$
1	−7.4977480097	−3.9929859616	−1.3949466718	−4.8646226839	−1.6964604732
2	−7.5116974764	−3.9969560931	−1.3949515364	−4.8646226839	−1.6964604732
3	−7.5117235260	−3.9969600484	−1.3949515364	−4.8646226839	−1.6964604732
4	−7.5117235747	−3.9969600523	−1.3949515364	−4.8646226839	−1.6964604732
> 5	−7.5117235748	−3.9969600523	−1.3949515364	−4.8646226839	−1.6964604732
Sum	−7.5117235748	−3.9969600523	−1.3949515364	−4.8646226839	−1.6964604732
N	$G_N^{-4}(\tau)$				
	$\tau = 1$ $(\times 10^{-5})$	$\tau = 1.1$ $(\times 10^{-5})$	$\tau = 2$ $(\times 10^{-10})$	$\tau = 4$ $(\times 10^{-21})$	$\tau = 6$ $(\times 10^{-32})$
1	5.62162252172	1.59439368892	1.94587621711	2.36645538565	2.87797813715
2	5.62164198041	1.59439526511	1.94587621713	2.36645538565	2.87797813715
3	5.62164198048	1.59439526512	1.94587621713	2.36645538565	2.87797813715
> 4	5.62164198048	1.59439526512	1.94587621713	2.36645538565	2.87797813715
Sum	5.62164198048	1.59439526512	1.94587621713	2.36645538565	2.87797813715
N	$G_N^{-6}(\tau)$				
	$\tau = 1$ $(\times 10^{-7})$	$\tau = 1.1$ $(\times 10^{-8})$	$\tau = 2$ $(\times 10^{-15})$	$\tau = 4$ $(\times 10^{-31})$	$\tau = 6$ $(\times 10^{-48})$
1	−4.2149509073	−6.3663916171	−2.7143935528	−1.1511912549	−4.8823761524
2	−4.2149509344	−6.3663916233	−2.7143935528	−1.1511912549	−4.8823761524
> 3	−4.2149509344	−6.3663916233	−2.7143935528	−1.1511912549	−4.8823761524
Sum	−4.2149509344	−6.3663916233	−2.7143935528	−1.1511912549	−4.8823761524

References

1. Dasgupta, A., Bhandarkar, S.M.: A generalized self-consistent Mori-Tanaka scheme for fiber-composites with multiple interphases. Mech. Mater. **14**, 67–82 (1992)
2. Benveniste, Y.: A new approach to the application of Mori-Tanaka's theory in composite materials. Mech. Mater. **6**, 147–157 (1987)
3. Jasiuk, I., Tong, Y.: Effect of interface on the elastic stiffness of composites. Am. Soc. Mech. Eng. Appl. Mech. Div. AMD. **100**, 49–54 (1989)
4. Hassan, S.A., Ahmed, H., Israr, A.: An Analytical Modeling for Effective Thermal Conductivity of Multi-Phase Transversely Isotropic Fiberous Composites Using Generalized Self-Consistent Method. Appl. Mech. Mater. **249–250**, 904–909 (2013)
5. Yan, P., Chen, F.L., Jiang, C.P., Song, F.: An eigenfunction expansion-variational method in prediction of the transverse thermal conductivity of fiber reinforced composites considering interfacial characteristics. Compos. Sci. Technol. **70**, 1726–1732 (2010)
6. Zhang, J., Eisenträger, J., Duczek, S., Song, C.: Discrete modeling of fiber reinforced composites using the scaled boundary finite element method. Compos. Struct. **235**, 111744 (2020)
7. Würkner, M., Berger, H., Gabbert, U.: On numerical evaluation of effective material properties for composite structures with rhombic fiber arrangements. Int. J. Eng. Sci. **49**, 322–332 (2011)
8. Jayachandran, K.P., Guedes, J.M., Rodrigues, H.C.: Homogenization method for microscopic characterization of the composite magnetoelectric multiferroics. Sci. Rep. **10**, 1276 (2020)
9. Rodríguez-Ramos, R., Sabina, F.J., Guinovart-Díaz, R., Bravo-Castillero, J.: Closed-form expressions for the effective coefficients of a fiber-reinforced composite with transversely isotropic constituents-I. Elastic and square symmetry. Mech. Mater. **33**, 223–235 (2001)
10. Pobedrya, B.E.: Mechanics of Composite Materials. Moscow State University Press (in Russian) (1984)
11. Dinzart, F., Sabar, H., Berbenni, S.: Homogenization of multi-phase composites based on a revisited formulation of the multi-coated inclusion problem. Int. J. Eng. Sci. **100**, 136–151 (2016)
12. Penta, R., Gerisch, A.: The asymptotic homogenization elasticity tensor properties for composites with material discontinuities. Contin. Mech. Thermodyn. **29**, 187–206 (2017)
13. López-López, E., Sabina, F.J., Guinovart-Díaz, R., Bravo-Castillero, J., Rodríguez-Ramos, R.: Overall longitudinal shear elastic modulus of a 1–3 composite with anisotropic constituents. Int. J. Solids Struct. **50**, 2573–2583 (2013)
14. Kolpakov, A., Kolpakov, A.: Capacity and Transport in Contrast Composite Structures: Asymptotic analysis and applications. CRC Press, Boca Raton (2009)
15. Bensoussan, A., Lions, J., Papanicolaou, G.: Asymptotic Analysis for Periodic Structures. North Holland (1978)

16. Jikov, V.V., Kozlov, S.M., Oleinik, O.A.: Homogenization of Differential Operators and Integral Functionals. Springer, Berlin (1994)
17. Sánchez-Palencia, E.: Non Homogeneous Media and Vibration Theory. Springer, Berlin (1980)
18. Allaire, G., Qatu, M.S.: Reviewer: shape optimization by the homogenization method. Applied Mathematical Sciences. Appl. Mech. Rev. **56**, B26–B27 (2003)
19. Firooz, S., Chatzigeorgiou, G., Meraghni, F., Javili, A.: Bounds on size effects in composites via homogenization accounting for general interfaces. Contin. Mech. Thermodyn. **32**, 173–206 (2020)
20. Oleinik, A., Panasenko, G.P., Yosifian, G.A.: Homogenization and asymptotic expansions for solutions of the elasticity system with rapidly oscillating periodic coefficients. Appl. Anal. **15**, 15–32 (1983)
21. Bakhvalov, N.S., Panasenko, G.P.: Homogenization Averaging Processes in Periodic Media. Kluwer Academic, Dordrecht (1989)
22. Guinovart-Díaz, R., Rodríguez-Ramos, R., Espinosa-Almeyda, Y., López-Realpozo, J.C., Dumont, S., Lebon, F., Conci, A.: An approach for modeling three-phase piezoelectric composites. Math. Methods Appl. Sci. **40**, 3230–3248 (2017)
23. Sabina, F.J., Guinovart-Díaz, R., Espinosa-Almeyda, Y., Rodríguez-Ramos, R., Bravo-Castillero, J., López-Realpozo, J.C.C., Guinovart-Sanjuán, D., Böhlke, T., Sánchez-Dehesa, J.: Effective transport properties for periodic multiphase fiber-reinforced composites with complex constituents and parallelogram unit cells. Int. J. Solids Struct. **204–205**, 96–113 (2020)
24. Espinosa-Almeyda, Y., Camacho-Montes, H., Otero, J.A., Rodríguez-Ramos, R., López-Realpozo, J.C., Guinovart-Díaz, R., Sabina, F.J.: Interphase effect on the effective magneto-electro-elastic properties for three-phase fiber-reinforced composites by a semi-analytical approach. Int. J. Eng. Sci. **154**, 103310 (2020)
25. Otero, J.A., Rodríguez-Ramos, R., Bravo-Castillero, J., Guinovart-Díaz, R., Sabina, F.J., Monsivais, G.: Semi-analytical method for computing effective properties in elastic composite under imperfect contact. Int. J. Solids Struct. **50**, 609–622 (2013)
26. Rodríguez-Ramos, R., Berger, H., Guinovart-Díaz, R., López-Realpozo, J.C., Würkner, M., Gabbert, U., Bravo-Castillero, J.: Two approaches for the evaluation of the effective properties of elastic composite with parallelogram periodic cells. Int. J. Eng. Sci. **58**, 2–10 (2012)
27. Muskhelishvili, N.I.: Some Basic Problems of the Mathematical Theory of Elasticity. Noordhoff, Groningen, Holland (1953)
28. Grigolyuk, E.I., Fil'shtinskii, L.A.: Perforated Plates and shells. M. Nauk (1970)
29. Sabina, F.J., Rodríguez-Ramos, R., Bravo-Castillero, J., Guinovart-Díaz, R., Guinovart-Díaz, R., Bravo-Castillero, J., Rodríguez-Ramos, R., Sabina, F.J., Rodríguez-Ramos, R., Bravo-Castillero, J., Guinovart-Díaz, R.: Closed-form expressions for the effective coefficients of a fibre-reinforced composite with transversely isotropic constituents. II. Piezoelectric and hexagonal symmetry. J. Mech. Phys. Solids. **49**, 1463–1479 (2001)
30. Mol'kov, V.A., Gurgova, O.É.: Moduli of elasticity of hybrid unidirectional fibrous composite. Mech. Compos. Mater. **22**, 703–706 (1987)
31. Rylko, N.: Effect of polydispersity in conductivity of unidirectional cylindres. Arch. Mater. Sci. Eng. **29**, 45–52 (2008)
32. Yan, P., Zhang, Z.A., Chen, F.L., Jiang, C.P., Wang, X.J., Qiu, Z.P.: Effective transport properties of composites with a doubly-periodic array of fiber pairs and with a triangular array of fibers. ZAMM J. Appl. Math. Mech. Z. Angew. Math. Mech. **98**, 312–329 (2018)
33. Mityushev, V.: Representative cell in mechanics of composites and generalized Eisenstein–Rayleigh sums. Complex Var. Elliptic Equ. **51**, 1033–1045 (2006)
34. Rayleigh, L.: On the influence of obstacles arranged in rectangular order upon the properties of a medium. Lond. Edinb. Dublin Philos. Mag. J. Sci. **34**(211), 481–502 (1982)
35. Berman, C.L., Greengard, L.: A renormalization method for the evaluation of lattice sums. J. Math. Phys. **35**, 6036–6048 (1994)
36. Huang, J.: Integral representations of harmonic lattice sums. J. Math. Phys. **40**, 5240–5246 (1999)
37. Ling, C.-B.: Evaluation at half periods of Weierstrass' elliptic function with rectangular primitive period-parallelogram. Math. Comput. **14**, 67–70 (1960)
38. Ling, C.-B., Tsai, C.-P.: Evaluation at Half Periods of Weierstrass' elliptic function with rhombic primitive period-parallelogram. Math. Comput. **18**, 433–440 (1964)
39. Ling, C.-B.: Evaluation at Half periods of Weierstrass' elliptic functions with double periods 1 and $e^{i\alpha}$. Math. Comput. **19**, 658–661 (1965)
40. Ling, C.B.: Tables of values of σ_2 relating to Weierstrass' elliptic function. Math. Comput. **19**, 123–127 (1965)
41. Movchan, A.B., Nicorovici, N.A., McPhedran, R.C.: Green's tensors and lattice sums for electrostatics and elastodynamics. Proc. R. Soc. Lond. Ser. A Math. Phys. Eng. Sci. **453**, 643–662 (1997)
42. Perrins, W., McKenzie, D., McPhedran, R.: Transport properties of regular arrays of cylinders. Proc. R. Soc. A Math. Phys. Eng. Sci. **369**, 207–225 (1979)
43. Rogosin, S., Dubatovskaya, M., Pesetskaya, E.: Eisenstein sums and functions and their application at the study of heat conduction in composites. Š'iauliai Math. Semin. **4**, 167–187 (2009)
44. Godin, Y.A.: The effective conductivity of a periodic lattice of circular inclusions. J. Math. Phys. **53**, 63703 (2012)
45. Godin, Y.A.: Effective properties of periodic tubular structures. Q. J. Mech. Appl. Math. **69**, 181–193 (2016)
46. Chen, P., Smith, M., McPhedran, R.: Evaluation and regularization of generalized Eisenstein series and application to 2D cylindrical harmonic sums. arXiv Math. Phys. (2016)
47. Borwein, J.M., Glasser, M.L., McPhedran, R.C., Wan, J.G., Zucker, I.J.: Lattice Sums Then and Now. Cambridge University Press, Cambridge (2013)
48. Yakubovich, S., Drygas, P., Mityushev, V.: Closed-form evaluation of two-dimensional static lattice sums. Proc. R. Soc. A Math. Phys. Eng. Sci. **472**, 20160510 (2016)
49. Cioranescu, D., Donato, P.: An Introduction to Homogenization. Oxford University Press, Oxford (2000)
50. López-Realpozo, J.C., Rodríguez-Ramos, R., Quintero Roba, A.J., Brito-Santana, H., Guinovart-Díaz, R., Tita, V., Lebon, F., Camacho-Montes, H., Espinosa-Almeyda, Y., Bravo-Castillero, J., Sabina, F.J.: Behavior of piezoelectric layered composites with mechanical and electrical non-uniform imperfect contacts. Meccanica **55**, 125–138 (2020)

51. Qiu, J., Tang, X., Chen, H., Liu, X., Hu, Z.: A tunable broadband magnetoelectric and electromagnetic hybrid vibration energy harvester based on nanocrystalline soft magnetic film. Surf. Coatings Technol. **320**, 447–451 (2017)
52. Rodriguez-Ramos, R., Guinovart-Díaz, R., López-Realpozo, J.C., Bravo-Castillero, J., Sabina, F.J., Lebon, F., Dumont, S., Berger, H., Gabbert, U., Wu, M.: Characterization of piezoelectric composites with mechanical and electrical imperfect contacts. J. Compos. Mater. **50**, 1–23 (2016)
53. Guinovart-Díaz, R., Rodríguez-Ramos, R., López-Realpozo, J.C., Bravo-Castillero, J., Otero, J.A., Sabina, F.J., Lebon, F., Dumont, S.: Analysis of fibrous elastic composites with nonuniform imperfect adhesion. Acta Mech. **227**, 57–73 (2016)
54. Hofer, U., Luger, M., Traxl, R., Lackner, R.: Closed-form expressions for effective viscoelastic properties of fiber-reinforced composites considering fractional matrix behavior. Mech. Mater. **127**, 14–25 (2018)
55. Markushevich, A.I.: Theory of Functions of a Complex Variable. Prentice-Hall (1967)
56. Corson, E.T.: An Introduction to the Theory of Funtions of a Complex Variable. Clarendon Press, Oxford (1935)
57. Weil, A.: Elliptic Functions according to Eisenstein and Kronecker. Springer, Berlin (1976)
58. López-Realpozo, J.C., Rodríguez-Ramos, R., Guinovart-Díaz, R., Bravo-Castillero, J., Otero, J.A., Sabina, F.J., Lebon, F., Dumont, S., Sevostianov, I.: Effective elastic shear stiffness of a periodic fibrous composite with non-uniform imperfect contact between the matrix and the fibers. Int. J. Solids Struct. **51**, 1253–1262 (2014)
59. Rodríguez-Ramos, R., Yan, P., López-Realpozo, J.C., Guinovart-Díaz, R., Bravo-Castillero, J., Sabina, F.J., Jiang, C.P.: Two analytical models for the study of periodic fibrous elastic composite with different unit cells. Compos. Struct. **93**, 709–714 (2011)
60. Espinosa-Almeyda, Y., Camacho-Montes, H., Rodríguez-Ramos, R., Guinovart-Díaz, R., López-Realpozo, J.C., Bravo-Castillero, J., Sabina, F.J.: Influence of imperfect interface and fiber distribution on the antiplane effective magneto-electro-elastic properties for fiber reinforced composites. Int. J. Solids Struct. **112**, 155–168 (2017)

Publisher's Note Springer Nature remains neutral with regard to jurisdictional claims in published maps and institutional affiliations.